High-Capacity Anode Materials for All-Solid-State Lithium Batteries

Reona Miyazaki*

Department of Physical Science and Engineering, Graduate School of Engineering, Nagoya Institute of Technology, Gokiso-cho, Showa-ward, Nagoya, Japan

This mini review article summarizes the recent progress of the all-solid-state lithium ion batteries (LIBs) with high-capacity anodes. Although the theoretical capacity of silicon (Si) is exceptionally high, the large volume change during cycling is a severe drawback for practical applications. The volume change of the active materials leads to mechanical degradation and electrical contact loss, resulting in a poor cycling performance. Recently, the number of reports about Si anodes in liquid electrolytes has significantly increased, leading to the better understanding of the electrochemical performances of Si. For the realization of the LIBs with a high capacity and safety, high-capacity alloy anodes are highly required to be used in all-solid-state batteries. However, at the present stage, research studies of high-capacity anodes with solid electrolytes are scarce compared to the vast amount of reports using liquid electrolyte. The selection of solid electrolytes is also a key factor for the stable performance of high-capacity anodes in the all-solid-state batteries, while previous studies on Si anodes have mainly focused on the fabrication of the hollow structured anodes for reducing their volume expansion. This review will provide some reports about the cycling properties of high-capacity anodes in the all-solid-state batteries and the solid electrolyte interface (SEI) formation at the anode interface of solid electrolytes. The potential of the high-capacity anodes for practical applications in all-solid-state batteries will be discussed.

Keywords: high-capacity anodes, all-solid-state lithium ion batteries, solid electrolytes, sulfides, solid electrolyte interphase

INTRODUCTION

Lithium ion batteries (LIBs) have been widely used as the power source of portable devices such as laptop personal computers (PCs) and smartphones. The lowest electrode potential of Li/Li$^+$ makes it possible to construct a high-voltage battery, which is the reason why LIBs are dominating the battery market. For the conventional LIBs, there are two major issues to overcome. One is the safety problem of the LIBs, which is frequently reported as the ignition of portable devices such as laptop PCs, smartphones, etc. These accidental fires of the LIBs originate from the flammable organic liquid used as the electrolyte. Because the anode potential of the LIBs is much lower than the reductive decomposition voltage of aqueous electrolytes, organic liquids are used as the electrolytes. The replacement of the organic liquid by a ceramic solid electrolyte is one of the solutions for the realization of safe LIBs. For this reason, all-solid-state batteries have attracted much attention as the

next-generation LIBs. The other issue of the LIBs is the demand for a higher capacity because LIBs have started to be used for large-scale applications such as electric vehicles (EVs) and smart grids. In order to realize the cruising distance of EVs comparable to that of gasoline-fueled vehicles, the capacity of the LIBs should be four to five times higher than the current LIBs. It is easily predicted that LIB fires will be much more severe for the larger batteries compared to the batteries for portable use. Therefore, all-solid-state LIBs having an exceptionally high capacity and high safety are strongly required for the future.

Group IV elements, such as silicon (Si), germanium (Ge), and tin (Sn), can store 4.4 mol of Li per unit molar (for example, $Li_{4.4}Si$ for Si) (John et al., 1982; Huggins, 1999; Park et al., 2010). These Li storage capacities correspond to 4,200, 1,600, and 990 mAh g^{-1} for the Si, Ge, and Sn, respectively. Despite the high capacity, practical examples of applications are scarce due to the following drawbacks. One of the issues of high-capacity anodes is their large volume expansion ($\sim$300%) during operation. The repetition of the large volume change results in the pulverization and disintegration of the active materials, leading to the low reversibility during cycling (Kim et al., 2005). The second problem is the repeated formation of solid electrolyte interface (SEI) layers at fresh cracks in the electrodes, which yields to the continuous growth of the electrode impedance (Inaba et al., 2005). In order to achieve stable charge–discharge cycling, the common strategies are to allow for accommodation of the volume expansions by the introduction of void spaces in the active materials (Feng et al., 2018; Shen et al., 2018). For example, an interconnected Si hollow nanosphere is capable of accommodating volume changes without pulverization and delivering an initial discharge capacity of 2,800 mAh g^{-1} with less than 0.08% capacity fading rate per cycle (Yao et al., 2011). A discharge capacity of 600 mAh g^{-1} can be obtained for over 100 cycles from a porous Si composite coated by a nitrogen-doped amorphous carbon (Zhang et al., 2018). Mesoporous Si with the pore size diameter of 20–35 nm exhibits an excellent cycling stability for 500 cycles (Kim et al., 2018). Because the void spaces included in these materials never contribute to the charge–discharge capacity, the anode materials with the hollow structures inevitably meet the trade-off between the net capacity and cycling stability. Although there have been vast amounts of research studies about high-capacity anodes in a liquid electrolyte, reports about the all-solid-state LIBs are less common. In a solid electrolyte, the dendrite growth of Li along the grain boundaries is a severe problem particularly under high-rate cycling (Nagao et al., 2013). The use of alloy anodes is one of the solutions for avoiding the Li dendrites because of the faster kinetics of the alloying reaction over the dendrite formation. Therefore, the practical use of high-capacity anodes is highly required in all-solid-state LIBs because of not only their high capacity but also avoiding the internal short circuit due to the Li dendrites.
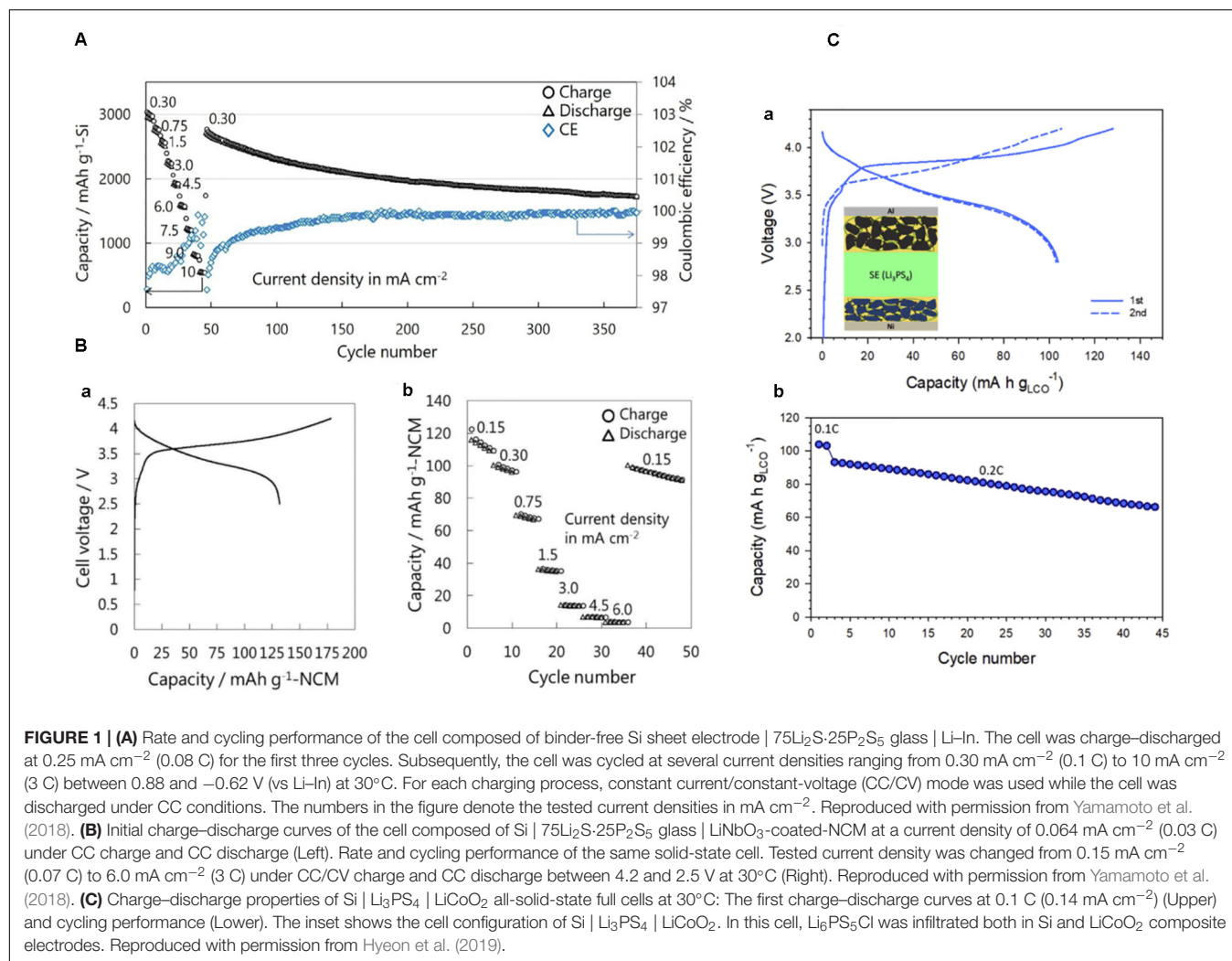
In this review, the electrode properties of high-capacity anodes in the all-solid-state LIBs are briefly reviewed. The solid electrolytes referenced in this review will focus exclusively on the sulfide-based materials. First, the reports about the Si-based thin film anodes in the all-solid-state LIBs are provided. Subsequently, the recent progress regarding the use of Si and Sn in a bulky form will be highlighted. Finally, the electrochemical and mechanical properties of the solid electrolytes will also be considered with cycling properties.

SILICON-BASED THIN-FILM ANODES IN THE ALL-SOLID-STATE LITHIUM ION BATTERIES

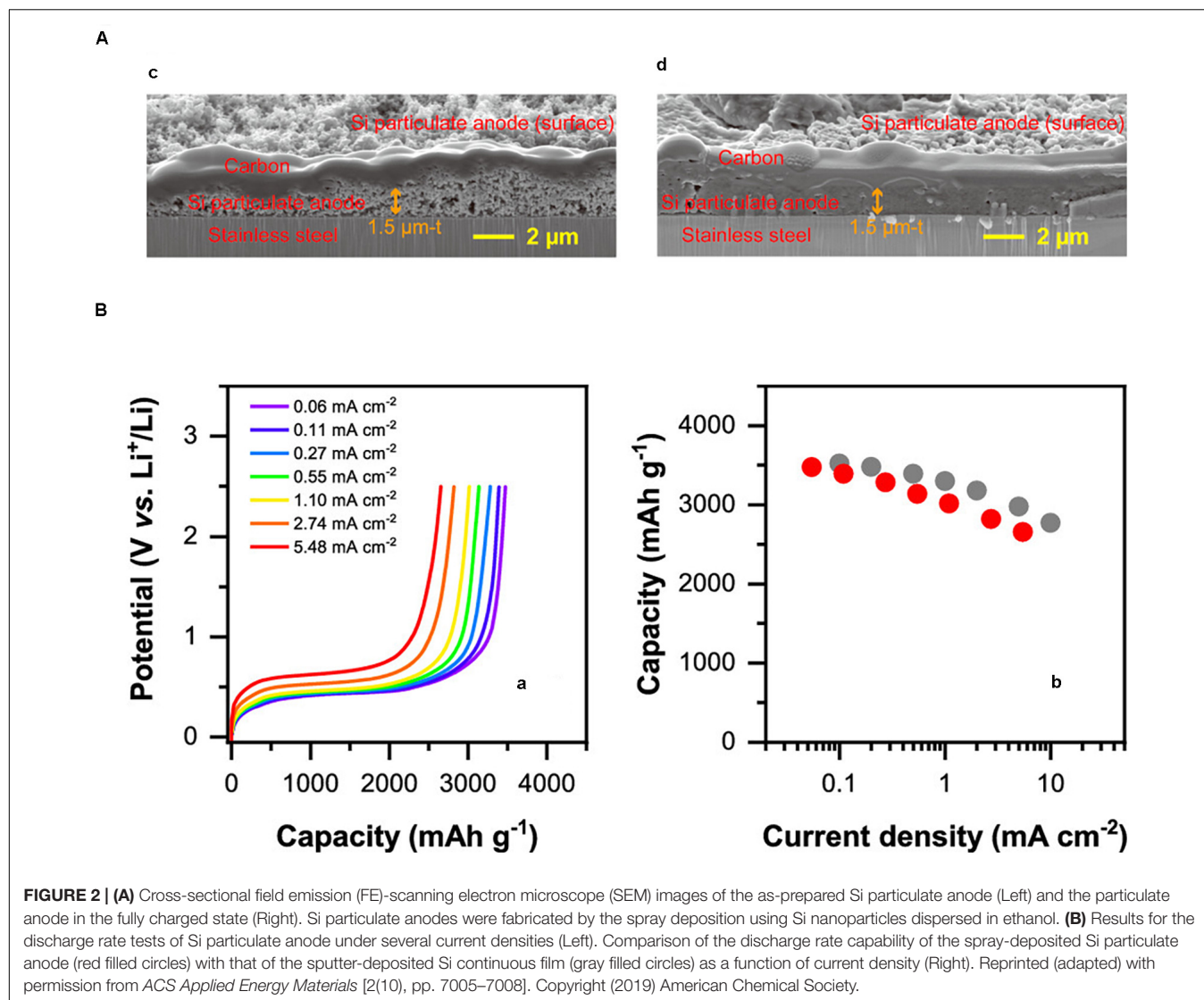## Silicon Thin-Film Anodes in the All-Solid-State Lithium Ion Batteries

For the all-solid-state LIBs with the sulfide solid electrolyte, the anode properties of Si have been initially reported and investigated in a thin film (Cervera et al., 2014; Miyazaki et al., 2014, 2016b; Sakabe et al., 2018). Because the net volume expansion is less than the bulk form, thin-film electrodes usually show better cycling properties compared to the bulky form (Takamura et al., 2004). In addition, the rate performance can be quantitatively investigated due to the easy determination of the electrode surface area. A Si thin film with FeS was fabricated by the pulsed laser deposition (PLD) method, and the charge–discharge properties were evaluated using a $70Li_2S\cdot30P_2S_5$ glass ceramic as the solid electrolyte (Mizuno et al., 2005), which revealed a stable cycling performance (Cervera et al., 2014). The most significant result is the discharge rate capability of the Si-FeS thin film; the capacity of 2,500 mAh g^{-1} was still maintained at the discharge rate of 10 C (Cervera et al., 2014). For this report, FeS was included as a conductive additive, while these excellent anode properties were also exhibited for sputtered a-Si films without additives (300 nm in thickness), in which the discharge capacity of 2,500 mAh g^{-1} was still maintained under 10 mA cm^{-2} and the charge transfer resistance between Si and $70Li_2S\cdot30P_2S_5$ was negligibly low (Miyazaki et al., 2014). These excellent properties originated from the use of solid electrolytes because the capacity fading was observed for the same a-Si film in a liquid electrolyte (Miyazaki et al., 2014). However, the active material loading in the 300-nm-thick film was only 70 μg cm^{-2} and provided an areal capacity of 0.21 mAh cm^{-2}, which is much lower than the typical values for commercial LIBs. Therefore, from an application point of view, thicker films are highly required. The excellent rate performances of Si films mean that Si-based anodes and the solid electrolytes can produce an intrinsically favorable interface and strongly indicate that the application of thicker films is possible if the interface is mechanically maintained during operation. In general, all-solid-state LIBs are fixed by screws and operating under a certain loading on the electrode and solid electrolyte layer. Therefore, it can be expected that the delamination of the Si film from the solid electrolyte and/or current collector would not be likely for the all-solid-state LIBs. However, the stable cycles of the thicker films are rather challenging for the dense Si film. The nonporous Si film of 3-μm thickness (0.70 mg cm^{-2}) gradually deteriorated and delivered only 47% of its 10th cycle's capacity (Sakabe et al., 2018). The nonporous Si film with its theoretical density was

FIGURE 1 | (A) Rate and cycling performance of the cell composed of binder-free Si sheet electrode | $75Li_2S \cdot 25P_2S_5$ glass | Li–In. The cell was charge–discharged at 0.25 mA cm^{-2} (0.08 C) for the first three cycles. Subsequently, the cell was cycled at several current densities ranging from 0.30 mA cm^{-2} (0.1 C) to 10 mA cm^{-2} (3 C) between 0.88 and −0.62 V (vs Li–In) at 30°C. For each charging process, constant current/constant-voltage (CC/CV) mode was used while the cell was discharged under CC conditions. The numbers in the figure denote the tested current densities in mA cm^{-2}. Reproduced with permission from Yamamoto et al. (2018). **(B)** Initial charge–discharge curves of the cell composed of Si | $75Li_2S \cdot 25P_2S_5$ glass | LiNbO$_3$-coated-NCM at a current density of 0.064 mA cm^{-2} (0.03 C) under CC charge and CC discharge (Left). Rate and cycling performance of the same solid-state cell. Tested current density was changed from 0.15 mA cm^{-2} (0.07 C) to 6.0 mA cm^{-2} (3 C) under CC/CV charge and CC discharge between 4.2 and 2.5 V at 30°C (Right). Reproduced with permission from Yamamoto et al. (2018). **(C)** Charge–discharge properties of Si | Li$_3$PS$_4$ | LiCoO$_2$ all-solid-state full cells at 30°C: The first charge–discharge curves at 0.1 C (0.14 mA cm^{-2}) (Upper) and cycling performance (Lower). The inset shows the cell configuration of Si | Li$_3$PS$_4$ | LiCoO$_2$. In this cell, Li$_6$PS$_5$Cl was infiltrated both in Si and LiCoO$_2$ composite electrodes. Reproduced with permission from Hyeon et al. (2019).

obtained by sputtering under Ar gas, while the pores of the size of 10–50 nm can be homogeneously introduced in Si film by using He as the sputtering gas (Sakabe et al., 2018). The nano porous Si film (0.74 mg cm^{-2}) exhibits stable cycling performances with the combination of $80Li_2S \cdot 20P_2S_5$ glass; the nano porous Si film delivered the high capacities of ~3,000 mAh g^{-1} and showed more than a 93% retention for 100 cycles compared to the capacity of 10 cycles, and the Coulombic efficiencies exceeded 99.8% (Sakabe et al., 2018). The areal capacity after 100 cycles was estimated to be 2.19 mAh cm^{-2}, which is a sufficiently high loading for practical use. Although it was suggested that the nano pores in the *a*-Si film can accommodate the volume expansion of Si, the pore volume was insufficient for covering all of the Si volume changes. Not only the void space in the Si film but also the favorable mechanical properties of the sulfide solid electrolyte will explain the stable cycling performance of the porous Si films in the all-solid-state LIBs. Li$_2$S-P$_2$S$_5$ glass systems exhibit a relatively low elastic modulus and thus might deform along with the Si volume change (Sakuda et al., 2013). At the present stage, there are few reports about Sn and Ge thin-film anodes for use in all-solid-state LIBs.

Anode Properties of Partially Oxidized and Nitrated Silicon Films

The low doping of oxygen leads to further enhancement of the discharge rate properties and cycling stability of the Si film (Miyazaki et al., 2016b). Generally, the doping of oxygen into the Si films stabilizes the cycling performance as the solid lithia matrix such that the reduction product during the initial charging process is believed to mechanically fix the active materials and prevent delamination (Courtney and Dahn, 1997). However, an excess amount of oxygen doping leads to an increased initial capacity loss, which means that there is a trade-off between the cycling stability and obtained capacity (Nguyen et al., 2013; Takezawa et al., 2013). The same trend was also found in the all-solid-state LIBs; however, the minimum amounts of oxygen required for the stable cycling are quite low in the solid electrolytes (SiO$_{0.4}$ film with the thickness of 300 nm); a discharge capacity of 2,800 mAh g^{-1} is still obtained after 100 cycles (Miyazaki et al., 2016b). Stable cycling was also attained for the SiN$_{0.92}$ film, although the capacity decreased to 700 mAh g^{-1} for the 500-nm-thick film (Suzuki et al., 2013).

FIGURE 2 | (A) Cross-sectional field emission (FE)-scanning electron microscope (SEM) images of the as-prepared Si particulate anode (Left) and the particulate anode in the fully charged state (Right). Si particulate anodes were fabricated by the spray deposition using Si nanoparticles dispersed in ethanol. **(B)** Results for the discharge rate tests of Si particulate anode under several current densities (Left). Comparison of the discharge rate capability of the spray-deposited Si particulate anode (red filled circles) with that of the sputter-deposited Si continuous film (gray filled circles) as a function of current density (Right). Reprinted (adapted) with permission from *ACS Applied Energy Materials* [2(10), pp. 7005–7008]. Copyright (2019) American Chemical Society.

HIGH-CAPACITY ANODES WITH POWDER MORPHOLOGY IN THE ALL-SOLID-STATE LITHIUM ION BATTERIES

Not only the thin film, but Si powder has also been started to be used in the all-solid-state LIBs (Arthur et al., 2018; Kato et al., 2018; Okuno et al., 2019). A slurry mixture consisting of Si, solid electrolytes, and acetylene black was shaken in a centrifuge tube with ZrO_2 balls and coated onto a carbon-coated copper foil electrode (Yamamoto et al., 2018). As shown in **Figure 1A**, the sheet Si electrode exhibited 3,100 mAh g^{-1} for the initial discharge with the Coulombic efficiency of 85%, which retained 2,300 mAh g^{-1} after 100 cycles (Yamamoto et al., 2018). Because the all-solid-state LIBs were fabricated by pressing at 75 MPa, the peel-off of Si can be avoided, which would partially explain the stable cycling performance of the Si sheet. Furthermore, the charge–discharge performances of the Si were evaluated using the

solid electrolytes with different Young's moduli (Kato et al., 2018). By doping with LiI, Young's modulus of the 75Li$_2$S·25P$_2$S$_5$ glass decreased from 23 to 19 GPa and the cycling stability was enhanced, although the conductivity of the solid electrolyte was not significantly changed (Kato et al., 2018). These results suggest that the applied pressure and the mechanical properties of the solid electrolytes should also be considered for the stable charge–discharge performances of the Si in the all-solid-state LIBs. A full cell composed of Si | 75Li$_2$S·25P$_2$S$_5$ glass | LiNbO$_3$-coated-LiNi$_{1/3}$Co$_{1/3}$Mn$_{1/3}$O$_2$ (NCM) and Si | Li$_3$PS$_4$ | LiCoO$_2$ was constructed and demonstrated stable charge–discharge cycling (**Figures 1B,C**) (Yamamoto et al., 2018; Hyeon et al., 2019). These results strongly indicated that Si is not prototype electrodes but have the potential to be actually incorporated in a practical cell. In a solid-state cell, the volume expansion of Si can be used to stabilize the cycle and rate performances while it should be avoided in the conventional LIBs with a liquid electrolyte. As shown in **Figure 2**, Si nano particles fabricated by spray deposition come into a continuous film after full charging, which

resulted in the excellent rate performances comparable to the sputter-deposited Si film electrode (Ohta et al., 2019).

Some research studies of the Sn anodes in a bulky form have also been reported. Polyacrylonitrile (PAN) was mixed with Sn nanoparticles as a conducting binder (Dunlap et al., 2019). The loading amount of the PAN binder was optimized (5 wt.%), the discharge capacity of 900 mAh g^{-1} was obtained for the first cycle, and 643 mAh g^{-1} was still maintained after 100 cycles at 0.1 C (Dunlap et al., 2019). It can be considered that Sn particles were electrochemically linked to the solid electrolyte particles and the current collector during cycling, whose rigid matrix contributed to the stable cycling (Dunlap et al., 2019). The use of the sheet style Sn anodes would be a significant step for the mass production of high-capacity all-solid-state LIBs. The commercially available Sn powder also works as an anode in the all-solid-state LIBs (Miyazaki and Hihara, 2019). A homogeneous composite electrode was obtained by the mechanical milling of Sn powder and $80Li_2S\cdot20P_2S_5$ glass, which resulted in excellent charge–discharge properties; the discharge capacity of 600 mAh g^{-1} was maintained for over 100 cycles (Miyazaki and Hihara, 2019). The conversion type electrode shows better cycling performances in a solid-state cell than in liquid electrolytes. SnS nanoparticles were fabricated by heating an oleylamine solution with sulfur and $SnCl_2$ at 230°C for 2 h, and the charge–discharge properties of the SnS were tested both in liquid and solid electrolytes ($77.5Li_2S\cdot22.5P_2S_5$ glass) (Kim et al., 2019a). Although the first discharge capacity in the liquid electrolyte (1,123 mAh g^{-1}) was higher than that in the solid electrolyte (802 mAh g^{-1}), the capacity decayed to 148 mAh g^{-1} after 50 cycles, while 85.6% of the discharge capacity at the second cycle was maintained for 100 cycles using the solid electrolyte (Kim et al., 2019a). The origin of the better properties in the solid-state cell can be explained by the reversibility of the conversion reaction. The discharge reaction of SnS consists of the conversion reaction of $SnS + 2Li^+ + 2e^- \rightarrow Li_2S + Sn$ followed by the alloying reaction of Sn. In the solid-state cell, the products of the conversion reaction (Li_2S) would reversely react with the Sn during the subsequent reconversion reaction while Li_2S was dissolved in the carbonate-based liquid electrolytes (Kim et al., 2019a). Hence, it is expected that the use of the solid electrolytes leads to a wider material selectivity of the anode materials. Li_2S was still found when the SnS-free cell was discharged to 1.0 V vs Li^+/Li. This Li_2S is believed to be the decomposition product of the sulfide-based solid electrolyte. The results of first-principles calculations indicated that the sulfide-based materials are not thermodynamically stable against Li, and the stability of the $Li_2S–P_2S_5$ systems is considered to be due to the sluggish kinetics of the decomposition reactions (Zhu et al., 2015). The decomposition products prevent further decomposition of the solid electrolytes, which is similar to the SEI layer formed at the anode interphase in the conventional LIBs. The decomposition products of the solid electrolytes were also experimentally observed in several research studies. For example, the SEI phase was formed between a Li-Al anode and the thio-LISICON ($Li_{3.25}Ge_{0.25}P_{0.75}S_4$) by applying a DC current to the symmetrical cell of Li-Al | thio-LISICON | Li-Al (Kanno et al., 2004). This SEI phase guaranteed an intimate contact

between the Li-Al/solid electrolyte and thus contributed to the stable charge–discharge cycling, while the formation of the SEI at the Li interface was continuous, thus the interfacial resistance continuously increased (Kanno et al., 2004). The SEI phases depend on the solid electrolytes; the SEI phase formed at the interphase of the Li–Al and $Li_3PO_4–Li_2S–SiS_2$ glass resulted in a high interfacial resistance (Kobayashi et al., 2008). Therefore, it can be said that not only the synthesis of anode materials but the selection of the solid electrolytes should also be considered for stable charge–discharge cycling.

SUMMARY AND PROSPECTS

In this mini review, the recent progresses of all-solid-state LIBs with high-capacity anodes were briefly reviewed. For the sulfide-based solid electrolytes, the stable cycling performances of Si and Sn have been shown in the bulky form. Although the material developments of high-capacity anodes have also been actively studied in liquid electrolytes, the material selectivity of the solid electrolytes will also be the key for the construction of the all-solid-state LIBs with Si and Sn. Although the $Li_2S-P_2S_5$ systems are not thermodynamically stable with Li-Sn, the stable SEI formation would result in the excellent cycling properties of SnS with $77.5Li_2S\cdot22.5P_2S_5$ glass (Kim et al., 2019a). It seems that the solid electrolytes with their favorable mechanical properties are required for the stable cycling of anodes by buffering the volume change of the active materials in a solid electrolyte layer. The external pressure of the cell should also be considered because the contact between the anodes and electrolytes would not be maintained during cycling without a certain degree of loading while an excessive applied pressure results in a limited capacity (Piper et al., 2013). Not only the sulfide materials but also hydride- and halide-based solid electrolytes have been developed and the conductivities of some materials have reached practical values (Miyazaki et al., 2016a; Kim et al., 2019b). The application of high-capacity anodes should not be restricted to only the sulfides, but other types of solid electrolytes have the potential to be used for the all-solid-state LIBs with high-capacity anodes. It should be noted that the conditions of the cell construction would depend on the types of solid electrolytes and should be optimized by considering both the mechanical properties and electrochemical stability of the solid electrolytes. It can be expected that the use of high-capacity alloy anodes will have a great contribution for increasing the energy density of the all-solid-state LIBs compatible with the safety of batteries.

AUTHOR CONTRIBUTIONS

The author confirms being the sole contributor of this work and has approved it for publication.

FUNDING

REFERENCES

Arthur, N., Kim, S., Jun, J., Hwan, K., and Lee, S. (2018). Simple and inexpensive coal-tar-pitch derived Si-C anode composite for all- solid-state Li-ion batteries. *Solid State Ionics* 324, 207–217. doi: 10.1016/j.ssi.2018.07.013

Cervera, R., Naoki, S., Tsuyoshi, O., Minoru, O., Kazutaka, M., Takayoshi, K., et al. (2014). High performance silicon-based anodes in solid-state lithium batteries. *Energy Environ Sci.* 7, 662–666. doi: 10.1039/c3ee43306d

Courtney, I. A., and Dahn, J. R. (1997). Electrochemical and in situ X-Ray diffraction studies of the reaction of Uthium with tin oxide composites. *J. Electrochem. Soc.* 144, 2045–2052.

Dunlap, N. A., Kim, J., Oh, K. H., and Lee, S. (2019). Slurry-coated sheet-style Sn-PAN anodes for all-solid-state li-ion batteries. *J. Electrochem. Soc.* 166, A915–A922. doi: 10.1149/2.0151906jes

Feng, K., Li, M., Liu, W., Kashkooli, A. G., Xiao, X., and Cai, M. (2018). Silicon-based anodes for lithium-ion batteries: from fundamentals to practical applications. *Small* 14:1702737. doi: 10.1002/smll.201702737

Huggins, R. A. (1999). Lithium alloy negative electrodes. *J. Power Sourc.* 81–82, 13–19. doi: 10.1016/s0378-7753(99)00124-x

Hyeon, D., Ah, H., Bae, Y., Woo, J., Lee, S., and Seok, Y. (2019). Sheet-type Li6PS5Cl-infiltrated Si anodes fabricated by solution process for all-solid-state lithium-ion batteries. *J. Power Sourc.* 426, 143–150. doi: 10.1016/j.jpowsour.2019.04.028

Inaba, M., Uno, T., and Tasaka, A. (2005). Irreversible capacity of electrodeposited Sn thin film anode. *J. Power Sourc.* 146, 473–477. doi: 10.1016/j.jpowsour.2005.03.052

John, M. R., St. Furgala, A. J., and Sammells, A. F. (1982). Thermodynamic studies of Li-Ge alloys: application to negative electrodes for molten salt batteries. *J. Electrochem. Soc.* 129, 246–250.

Kanno, R., Murayama, M., Inada, T., and Kobayashi, T. (2004). A Self-assembled breathing interface for all-solid-state ceramic lithium batteries. *Electrochem. Solid State Lett.* 7, A455–A458.

Kato, A., Yamamoto, M., Sakuda, A., Hayashi, A., and Tatsumisago, M. (2018). Mechanical properties of Li2S – P2S5 glasses with lithium halides and application in all-solid-state batteries. *ACS Appl. Energy Mater.* 1, 1002–1007. doi: 10.1021/acsaem.7b00140

Kim, J. W., Ryu, J. H., Lee, K. T., and Oh, S. M. (2005). Improvement of silicon powder negative electrodes by copper electroless deposition for lithium secondary batteries. *J. Power Sourc.* 147, 227–233. doi: 10.1016/j.jpowsour.2004.12.041

Kim, N., Park, H., Yoon, N., and Lee, J. K. (2018). Zeolite-templated mesoporous silicon particles for advanced lithium-ion battery anodes. *ACS Nano* 12, 3853–3864. doi: 10.1021/acsnano.8b01129

Kim, S., Choi, J., Bak, S., Sang, L., Li, Q., and Patra, A. (2019a). Reversible conversion reactions and small first cycle irreversible capacity loss in metal sulfide-based electrodes enabled by solid electrolytes. *Adv. Funct. Mater.* 2019:1901719. doi: 10.1002/adfm.201901719

Kim, S., Oguchi, H., Toyama, N., Sato, T., Takagi, S., and Otomo, T. (2019b). A complex hydride lithium superionic conductor for high-energy-density all-solid-state lithium metal metal batteries. *Nat. Commun* 10, 1–9. doi: 10.1038/s41467-019-09061-9069

Kobayashi, T., Yamada, A., and Kanno, R. (2008). Interfacial reactions at electrode / electrolyte boundary in all solid-state lithium battery using inorganic solid electrolyte, thio-LISICON. *Electrochim. Acta* 53, 5045–5050. doi: 10.1016/j.electacta.2008.01.071

Miyazaki, R., and Hihara, T. (2019). Charge-discharge performances of Sn powder as a high capacity anode for all-solid-state lithium batteries. *J. Power Sourc.* 427, 15–20. doi: 10.1016/j.jpowsour.2019.04.068

Miyazaki, R., Kurihara, D., and Hihara, T. (2016a). Li+ ionic conduction properties on NaI doped with a small amount of LiBH4. *J. Solid State Electrochem.* 20, 2759–2764. doi: 10.1007/s10008-016-3287-3

Miyazaki, R., Ohta, N., Ohnishi, T., and Takada, K. (2016b). Anode properties of silicon-rich amorphous silicon suboxide films in all-solid-state lithium batteries. *J. Power Sourc.* 329, 41–49. doi: 10.1016/j.jpowsour.2016.08.070

Miyazaki, R., Ohta, N., Ohnishi, T., Sakaguchi, I., and Takada, K. (2014). An amorphous Si film anode for all-solid-state lithium batteries. *J. Power Sourc.* 272, 541–545. doi: 10.1016/j.jpowsour.2014.08.109

Mizuno, F., Hayashi, A., Kiyoharu, T., and Tatsumisago, M. (2005). New, highly ion-conductive crystals precipitated from Li2S - P2S5 glasses. *Adv. Mater.* 17, 918–921. doi: 10.1002/adma.200401286

Nagao, M., Hayashi, A., Tatsumisago, M., Kanetsuku, T., Tsuda, T., and Kuwabata, S. (2013). In situ SEM study of a lithium deposition and dissolution mechanism in a bulk-type solid-state cell with a Li2S-P2S5 solid electrolyte. *Phys. Chem. Chem. Phys.* 15, 18600–18606. doi: 10.1039/c3cp51059j

Nguyen, C. C., Choi, H., and Song, S. (2013). Roles of oxygen and interfacial stabilization in enhancing the cycling ability of silicon oxide anodes for rechargeable lithium batteries. *J. Electrochem. Soc.* 160, 906–914. doi: 10.1149/2.118306jes

Ohta, N., Kimura, S., Sakabe, J., Mitsuishi, K., Ohnishi, T., and Takada, K. (2019). Anode properties of Si nanoparticles in all-solid-State Li batteries. *ACS Appl. Energy Mater.* 2, 7005–7008. doi: 10.1021/acsaem.9b01517

Okuno, R., Yamamoto, M., Terauchi, Y., and Takahashi, M. (2019). Stable cyclability of porous Si anode applied for sulfide-based all-solid-state batteries. *Energy Proc.* 156, 183–186. doi: 10.1016/j.egypro.2018.11.125

Park, C., Kim, J., Sohn, H., Park, C., and Kim, J. (2010). Li-alloy based anode materials for Li secondary batteries. *Chem. Soc. Rev.* 39, 3115–3141. doi: 10.1039/b919877f

Piper, D. M., Yersak, T. A., and Lee, S. (2013). Effect of compressive stress on electrochemical performance of silicon anodes. *J. Electrochem. Soc.* 160, A77–A81. doi: 10.1149/2.064301jes

Sakabe, J., Ohta, N., Ohnishi, T., Mitsuishi, K., and Takada, K. (2018). Porous amorphous silicon film anodes for high-capacity and stable all-solid-state lithium batteries. *Commun. Chem.* 1, 1–9.

Sakuda, A., Hayashi, A., and Tatsumisago, M. (2013). Sulfide solid electrolyte with favorable mechanical property for all-solid-state lithium battery. *Sci. Rep.* 3, 1–5. doi: 10.1038/srep02261

Shen, T., Yao, Z., Xia, X., Wang, X., Gu, C., and Tu, J. (2018). Rationally designed silicon nanostructures as anode material for lithium-ion batteries. *Adv. Energy Mater.* 20:1700591. doi: 10.1002/adem.201700591

Suzuki, N., Cervera, L., Butch, R., Ohnishi, T., and Takada, K. (2013). Silicon nitride thin film electrode for lithium-ion batteries. *J. Power Sourc.* 231, 186–189. doi: 10.1016/j.jpowsour.2012.12.097

Takamura, T., Ohara, S., Uehara, M., Suzuki, J., and Sekine, K. (2004). A vacuum deposited Si film having a Li extraction capacity over 2000 mAh/g with a long cycle life. *J. Power Sourc.* 129, 96–100. doi: 10.1016/j.jpowsour.2003.11.014

Takezawa, H., Iwamoto, K., Ito, S., and Yoshizawa, H. (2013). Electrochemical behaviors of nonstoichiometric silicon suboxides (SiOx) film prepared by reactive evaporation for lithium rechargeable batteries. *J. Power Sourc.* 244, 149–157. doi: 10.1016/j.jpowsour.2013.02.077

Yamamoto, M., Terauchi, Y., Sakuda, A., and Takahashi, M. (2018). Slurry mixing for fabricating silicon-composite electrodes in all-solid-state batteries with high areal capacity and cycling stability. *J. Power Sourc.* 402, 506–512. doi: 10.1016/j.jpowsour.2018.09.070

Yao, Y., Mcdowell, M. T., Ryu, I., Wu, H., Liu, N., Hu, L., et al. (2011). Interconnected silicon hollow nanospheres for lithium-ion battery anodes with long cycle life. *Nano Lett.* 11, 2949–2954. doi: 10.1021/nl201470j

Zhang, C., Cai, X., Chen, W., Yang, S., Xu, D., Fang, Y., et al. (2018). 3D Porous Silicon/N-doped carbon composite derived from bamboo charcoal as high-performance anode material for lithium- ion batteries. *ACS Sustain. Chem. Eng.* 6, 9930–9939. doi: 10.1021/acssuschemeng.8b01189

Zhu, Y., He, X., and Mo, Y. (2015). Origin of outstanding stability in the Lithium solid electrolyte materials: insights from thermodynamic analyses based on first-principles calculations. *ACS Appl. Mater. Interf.* 7, 23685–23693. doi: 10.1021/acsami.5b07517